Supplementary Methods:

A neuron autonomous role for the Familial Dysautonomia gene ELP1 in sympathetic and sensory target tissue innervation.

Marisa Z. Jackson, Katherine A. Gruner, Charles Qin and Warren G. Tourtellotte

Generating Elp1-flx mice: A 6.6 kb C57BL/6 mouse genomic DNA fragment of the elp1 gene (nt 5766-12423, Genbank AL807762) was isolated from mouse BAC clone RP23-155E17 (Chori, Oakland CA) using gap repair and homologous recombination in E. Coli (Liu et al. 2003). A forward oriented loxP site flanked by EcoRI and BamHI sites was targeted into intron 19 (nt 8934, Genbank AL807762) and a PGK-Neo (Neo) positive-selection cassette flanked by Frt sites and a 3' forward oriented loxP site was targeted into intron 20 (nt 9299, Genbank AL807762) using recombineering to generate the final targeting construct (Liu et al. 2003). The targeting construct was electroporated into isogenic C57/BL6 ES cells and genomic DNA from G418-resistant clones was screened for homologous recombination. G418 resistant ES cell clones were initially screened using long-range PCR flanking the 3' recombination arm of the targeting construct with primers OT1589 (ATAGGAACTTCATCAGTCAG) and OT1590 (TGGAATAATGACTAACCTCT) to generate a 3.2 kb amplicon indicating a targeted 3' recombination event. PCR-positive clones were additionally screened by Southern blotting with a 685 nt probe located 5' of the 5' recombination arm (spanning nt 4757-5442, Genbank AL807762) that was hybridized to NheI endonuclease restricted ES cell genomic DNA to yield a 7.8 kb wild type allele band and a 5.3 kb targeted allele band in appropriately recombined clones. Six properly targeted clones were identified and three were injected into isogenic C57BL/6J blastocysts using standard methods (Magin et al. 1992). Chimeric mice were mated to C57BL/6J female mice and germline heterozygote mice ($Elp1^{+/Neo}$) were identified. Germline $elp1^{+/Neo}$ heterozygous mice were mated to isogenic BL/6 CAG-

FlpE mice (Kanki et al. 2006) to remove the frt-flanked Neo positive-selection cassette from the germline and to generate the final Elp1-flx allele (designated $elp1^{+/f}$).

Elp1-flx mice were genotyped using primers: OT1623: 5'-CTGTGCCCCCTGCTGCTTAGAGGATCTCCAGTTGAT-3' and OT1652: 5'-CATAAGTCTGTGAGGACAGG-3' and standard PCR conditions.

Timed matings for embryonic analysis

Female mice were mated to male mice each day and checked for insemination plugs in the early morning. Females with plugs were considered to be impregnated at midnight and therefore considered to be at gestational age E0.5 in the morning after mating. Females with interval weight gain were determined to be pregnant and the embryos were harvested at E12.5.

Antibody reagents

Primary antibodies used for immunohistochemistry: Tyrosine hydroxylase (TH; Rabbit anti-TH, 1:5000, Chemicon), Ki67 (Rabbit anti-Ki67, 1:32500, Dako, Clone Tek-3), cleaved caspase 3 (CC3; Rabbit anti-CC3, 1:500, Cell Signaling), peripherin (Prph; Rabbit anti-Prph, 1:1000, Millipore), neurofilament heavy chain (NF-H; Rabbit anti-NF200, 1:1000, Millipore), parvalbumin (Pv; Goat anti-Pv, 1:1000, Swant), renin (Rn; goat anti-renin, 1:150, Santa Cruz), elp1 (elp1; Rabbit anti-elp1/IKAP, 1:200 tissue section and 1:1000 on cells in culture, LSBio), tyrosinated alpha-tubulin (Y-αTub; Rat anti-Y-αTub, 1:6000, Serotec), acetylated alpha-tubulin (Ac-αTub; Mouse anti-Ac-αTub, 1:6000, Sigma), TrkA (Tropomyosin related kinase A (Ntrk1), Rabbit anti-TrkA, 1:1000, Millipore), TrkB (Tropomyosin related kinase B (Ntrk2), Goat anti-TrkA, 1:1000, R&D Systems), TrkC (Tropomyosin related kinase C (NTrk3), Goat anti-TrkC, 1:1000, R&D Systems), SCG10 (Stmn2, Rabbit anti-stmn2, 1:1000, Millipore), or NPY (Neuropeptide Y, Rabbit anti-NPY, 1:1000, Millipore) was performed on either frozen or paraffin embedded tissue sections. βIII tubulin immunocytochemistry (Tuj1; Mouse anti-tubulin, TU-20, 1:500, Chemicon) was used to label neurons grown in culture.

Immunohistochemistry

Immunohistochemical staining was performed using antigen specific primary antibodies and species appropriate secondary antibodies conjugated to Cy3 (Jackson Immunoresearch, West Grove, PA) or Alexa488 (Invitrogen, Grand Island, NY) were used to localize primary antibody binding by immunofluorescence and 4',6-diamidino-2-phenylindole (DAPI) was used as a fluorescent nuclear counterstain. In some experiments, species appropriate secondary antibodies conjugated to horseradish peroxidase (HRP) and 3, 3'-diaminobenzidine (DAB) as a chromogen were used to localize the primary antibody with standard methods. For all antibodies, non-immune serum was used in place of the primary antibody to control for non-specific antibody binding.

Western Blotting

Cells or tissues were lysed in RIPA buffer (20 mM Tris, pH 7.7, 150 mM NaCl, 1% NP-40, 0.5% sodium deoxycholate, 0.1% SDS) supplemented with 10 nM NaF and Complete protease inhibitors (Roche, Alameda, CA). Twenty micrograms of total cellular protein was resolved by SDS-PAGE on a 4-20% acrylamide gel and transferred to a nitrocellulose membrane. Blots were probed for elp1 (Rabbit anti-Elp1, 1:2000, Sigma) followed by a horseradish peroxidase-conjugated goat anti-rabbit secondary antibody (Jackson ImmunoResearch, West Grove, PA) and visualized using SuperSignal West Femto chemiluminescent substrate (Pierce, Rockford, IL). Relative elp1 quantification was assessed by measuring fluorescence intensity (VersaDoc, Bio-Rad, Hercules, CA) on Western blots in the linear range of chemiluminescent detection from three independent experiments.

Whole-mount TH-immunohistochemistry

Representative sympathetic target tissues including stomach, submandibular salivary gland, kidney, heart, spleen and bowel were isolated from paraformaldehyde perfused newborn Wnt1-Ctl (Wnt1-Cre^{+}; elp1$^{+/+}$), DβH-Ctl (DβH-iCre^{+};elp1$^{+/+}$), Wnt1-cKO (Wnt1-Cre^{+}; elp1$^{f/f}$) and DβH-cKO (DβH-iCre^{+}; elp1$^{f/f}$) mice using previously published methods (Enomoto et al. 2001; Glebova and Ginty 2004). To

improve visualization of TH+ sympathetic axons deep within tissues, dehydration in methanol and clearing by overnight immersion in a solution of 2:1 benzyl benzoate/benzyl alcohol was performed.

In vivo semi-quantitative sensory and sympathetic target innervation and axon bundle branching using fluorescence immunohistochemistry

Representative and comparable target tissues such as foot pads for evaluating cutaneous Prph- and NF-H-positive sensory axon innervation and submandibular salivary gland, spleen, heart, kidney and stomach for evaluating TH-positive sympathetic axon innervation were analyzed in areas with the highest innervation density in control tissues. The relative innervation was expressed as a mean percent (% Ctl) of the innervation observed in Wnt1-cKO or DβH-cKO normalized to the values obtained from Wnt1-Ctl or DβH-Ctl tissues using 3 animals of each genotype. To quantify proprioceptive innervation of skeletal muscle stretch receptors, Pv+ annulospiral terminal axon profiles on spindle stretch receptors (Tourtellotte and Milbrandt 1998) were counted in similar hindlimb muscles per tissue section in three separate animals of each genotype. The results were expressed as mean number of Pv+ terminal axon innervated spindle profiles observed in Wnt1-cKO and normalized to the results from Wnt-Ctl mice.

In vivo semi-quantitative sympathetic axon bundle branching using whole mount TH immunohistochemistry

Sympathetic axon branching in tissues stained using whole mount TH immunohistochemistry was evaluated using comparable digital images in control (Ctl) and cKO tissues by counting the number of axon branch points in a defined area. 6-8 images were examined from comparable regions in various target tissues from 3 animals of each genotype. The results were expressed as %Ctl by calculating the ratio of the number of axon branch points/unit area in cKO tissues relative to Ctl tissues.

LacZ enzyme histochemistry

Whole mount lacZ enzyme histochemistry was performed on tissues from newborn Wnt1-Ctl (Wnt1-Cre^{+}; elp1$^{+/+}$), DβH-Ctl (DβH-iCre^{+};elp1$^{+/+}$), Wnt1-cKO (Wnt1-Cre^{+}; elp1$^{f/f}$) and DβH-cKO (DβH-iCre^{+}; elp1$^{f/f}$) mice. Tissues were dissected and postfixed in 2% PFA, 0.2% glutaraldehyde, 5mM EGTA, 0.01% NP-40 in PBS-Mg at 4°C and reacted 6-8 hours at 37°C in reaction buffer (1mg/mL X-

gal, 5mM potassium ferrocyanide, 5mM potassium ferricyanide). Tissues were cleared by dehydrating in methanol and overnight immersion in a solution of 2:1 benzyl benzoate/benzyl alcohol. The tissues were imaged with a Nikon SMZ1500 stereomicroscope and a Nikon DS-Ri1 digital camera. Focal image planes were projected into single z-stack flat-field images using Zerene Stacker software (Zerene Systems LLC, Richland, WA).

In vivo ganglion neuron counts

Immunohistochemistry on either embryonic (E12.5) or newborn (P0) tissue sections containing SCG or thoracic (T1) DRG was performed using antibodies to Ki67, CC3, Prph or NF-H on every fourth serial 4 μm paraffin section as previously described (Albert et al. 2005; Eldredge et al. 2008; Quach et al. 2013). Digital images were obtained and neurons containing clearly visible nucleoli were counted in the DRG and SCG to ensure counting only a single neuron once across multiple sections. Sections spanning the entire rostral-caudal extent of the ganglia were analyzed and the sum of all counted neurons was considered an unbiased estimate of the total number of neurons within the ganglia.

Primary sympathetic neuron and dorsal root ganglion neuron cultures

SCG sympathetic and DRG sensory neurons from newborn (P0) $elp1^{+/+}$ and $elp1^{f/f}$ mice were isolated for neuron culture. Briefly, ganglionic neurons were dissociated with Type IV Collagenase (1 mg/ml, Sigma), followed by 0.25% Trypsin-EDTA and plated on poly-L-lysine (1 mg/mL, Sigma) and laminin (10 μg/mL, Sigma) coated German glass coverslips with media containing DMEM and 10% fetal bovine serum (FBS). Two hours after plating, additional media containing DMEM, 10% fetal bovine serum and 10 ng/mL NGF was added to the cultures. The neurons were differentiated for 2 days as previously described (Eldredge et al. 2008; Quach et al. 2013).

Neuron transfection and neurite outgrowth assays

Wild type neurons were nucleofected (Lonza, Basel Switzerland) with plasmids expressing enhanced green fluorescent protein (eGFP) and small hairpin RNA (shRNA) molecules targeting either mouse elp1 (shmelp1a, shmelp1b) or no specific sequence (shscramble). For rescue studies a plasmid was

used that expresses both red fluorescent protein (RFP) and human Elp1 (help1) that is not targeted by the mouse-sequence specific shRNA molecules. Functional knockdown of elp1 message by the shRNA molecules was previously characterized (Creppe et al. 2009) and reconfirmed in N2a mouse neuroblastoma cells (Fig. S8). In some experiments neurons isolated from $elp1^{+/+}$ and $elp1^{f/f}$ mice were infected with Adenovirus expressing eGFP and Cre-recombinase prior to plating. Neurite outgrowth parameters were measured using Metamorph software on calibrated digital images of βIII tubulin immunostained neurons that expressed eGFP as a marker of either viral infection or plasmid nucleofection. When help1 rescue experiments were used, co-transfected neurons that were both eGFP- and RFP-positive were analyzed. Neuron processes were traced using the DrawingSlate II drawing pad with TabletWorks software (GTCO CalComp peripherals, Scottsdale, AZ, USA) and neurite outgrowth and branching were quantified using Metamorph software on calibrated images. Total neurite length and the number of branch points were quantified for all neurites emanating from single neurons. The results were expressed as a percent of the mean values of knockout (KO) relative to Ctl neurons.

In vitro neuron survival assays

$elp1^{+/+}$ and $elp1^{f/f}$ SCG and DRG neurons were isolated and differentiated in the presence of 0.1, 1 and 10 ng/mL of NGF. Neurons were infected with Adenovirus expressing eGFP and Cre-recombinase. 48 hours after infection, the percent of neuron death was determined by counting the percent of infected (eGFP+) neurons that were apoptotic as determined by immunolabeling for CC3.

Semi-quantitative Ac-αTub and Y-αTub assay:

$elp1^{+/+}$ and $elp1^{f/f}$ SCG neurons were dissociated and infected with Adenovirus expressing eGFP and Cre-recombinase prior to plating. Twenty four hours after plating and differentiation, neurons were fixed and processed for immunocytochemistry using Ac-αTub and Y-αTub antibodies, and a Cy3-labeled secondary antibody. Fixation to analyze Ac-aTub was performed using 4% paraformaldehyde/0.1 M PB (pH=7.4) and for Y-Tub staining the cells were fixed with 100% methanol

at -20 deg. Infected neurons that expressed eGFP were analyzed for Ac-αTub and Y-αTub Cy3 fluorescence intensity using digital images acquired from either a Nikon E100 fluorescence microscope (AcTub) or a Zeiss Apoptome (Y-tub) with identical camera settings. The fluorescence intensity measurements were obtained using Metamorph and normalized to the cell body area. The mean normalized intensity in KO relative to Ctl neurons was quantified from triplicate experiments and greater than 50 randomly selected neurons analyzed per genotype.

Reverse transcriptase (RT)-PCR and gene expression (qPCR) analysis

Dissociated elp1$^{+/+}$ and elp1$^{f/f}$ sympathetic (SCG) and dorsal root ganglion neurons from newborn mice were differentiated in the presence of NGF (50 ng/ml) for 3 days. The neurons were infected at DIV3 with adenovirus that expressed both eGFP and Cre-recombinase, resulting in >95% infection efficiency. Total cellular RNA was isolated 48 hours after infection using Trizol (Invitrogen, Carlsbad, CA) and 1.0 μg of RNA was reverse transcribed using random octomer priming and Superscript III reverse transcriptase according to the manufacturer's specifications (Invitrogen). Exon 20 deletion in Cre-recombinase expressing elp1$^{f/f}$ neurons using oligos: OT1711 (CAGTGGAGAAATTCTGCG) and OT1714 (CACTCTTGGTAATCGGGG).

Gene expression analysis was performed using qPCR with probe-primer nuclease assays and an ABI StepOne Plus real-time PCR instrument. The FAM-labeled probes were designed to hybridize to exon-exon boundaries in cDNA to prevent the possibility of amplifying contaminating genomic DNA. The primer and probe sequences used are indicated: Stmn2/SCG10: probe: CCTTGTAGGCCATTGCTGTTTTAGCC, sense primer: GACCCTTCTCCTTTGCCTTC, anti-sense primer: TATGCTGTCACTGATCTGCTC. Rest: probe: ACTCACACAGGAGAACGCCCGTATA, sense primer: GATGAGTCTTCTGAGAGCTTGAG, anti-sense primer: GCAGCAAGTGCAACTACTTC. GAPDH: probe: TGCAAATGGCAGCCCTGGTG, sense primer: AATGGTGAAGGTCGGTGTG, anti-sense primer: GTGGAGTCATACTGGAACATGTAG. For

GAPDH expression, although the probe hybridized to exon 3, no genomic DNA was amplifiable because the primers span intron 2 which is too large for efficient amplification. Standard curves were generated for each probe/primer combination using pooled SCG and DRG neuron cDNA and the relative target gene expression results were normalized to GAPDH expression for each sample analyzed. Gene expression results were represented as the GAPDH normalized expression in $elp1^{f/f}$ neurons infected with Cre-recombinase expressing adenovirus relative to control (Ctl; $elp1^{+/+}$ neurons infected with Cre-recombinase expressing adenovirus). The results represented the mean of replicates from neurons isolated from 3 different cultures and compared using paired t-test.

Alizarin red and Alcian blue staining of bone and cartilage

Newborn pups were perfused with PFA and then post-fixed in 80% ethanol for a minimum of 24 hours prior to removing skin and visceral organs. The tissues were dehydrated in 96% ethanol for 1-3 days followed by 100 % acetone for 1-3 days. The tissues were stained overnight in 0.01% Alizarin red, 0.03% Alcian blue and 0.01% acid-alcohol. Tissue destaining and clearing were performed by sequential incubation in 95% ethanol, 1% aqueous potassium hydroxide (KOH), 20% glycerol in 1% KOH, 50% glycerol in 1% KOH, 80% glycerol in 1% KOH and placed into 100% glycerol for prolonged storage and imaging.

Statistical Measurements

All values were expressed as mean ± SEM and when individual groups were compared, Student's t-test was used to compare the means. In some cases data were analyzed using repeated measures ANOVA with genotype or treatment effect as the grouping variable. In all instances $p < 0.05$ was considered statistically significant.

References:

Albert Y, Whitehead J, Eldredge L, Carter J, Gao X, Tourtellotte WG. 2005. Transcriptional regulation of myotube fate specification and intrafusal muscle fiber morphogenesis. *J Cell Biol* **169**: 257-268.

Creppe C, Malinouskaya L, Volvert ML, Gillard M, Close P, Malaise O, Laguesse S, Cornez I, Rahmouni S, Ormenese S et al. 2009. Elongator Controls the Migration and Differentiation of Cortical Neurons through Acetylation of alpha-Tubulin. *Cell*.

Eldredge LC, Gao XM, Quach DH, Li L, Han X, Lomasney J, Tourtellotte WG. 2008. Abnormal sympathetic nervous system development and physiological dysautonomia in Egr3-deficient mice. *Development* **135**: 2949-2957.

Enomoto H, Crawford PA, Gorodinsky A, Heuckeroth RO, Johnson EM, Jr., Milbrandt J. 2001. RET signaling is essential for migration, axonal growth and axon guidance of developing sympathetic neurons. *Development* **128**: 3963-3974.

Glebova NO, Ginty DD. 2004. Heterogeneous requirement of NGF for sympathetic target innervation in vivo. *J Neurosci* **24**: 743-751.

Kanki H, Suzuki H, Itohara S. 2006. High-efficiency CAG-FLPe deleter mice in C57BL/6J background. *Exp Anim* **55**: 137-141.

Liu P, Jenkins NA, Copeland NG. 2003. A highly efficient recombineering-based method for generating conditional knockout mutations. *Genome research* **13**: 476-484.

Magin TM, McWhir J, Melton DW. 1992. A new mouse embryonic stem cell line with good germ line contribution and gene targeting frequency. *Nucleic Acids Res* **20**: 3795-3796.

Quach DH, Oliveira-Fernandes M, Gruner KA, Tourtellotte WG. 2013. A sympathetic neuron autonomous role for Egr3-mediated gene regulation in dendrite morphogenesis and target tissue innervation. *J Neurosci* **33**: 4570-4583.

Tourtellotte WG, Milbrandt J. 1998. Sensory ataxia and muscle spindle agenesis in mice lacking the transcription factor Egr3. *Nat Genet* **20**: 87-91.

Supplementary Figure 1

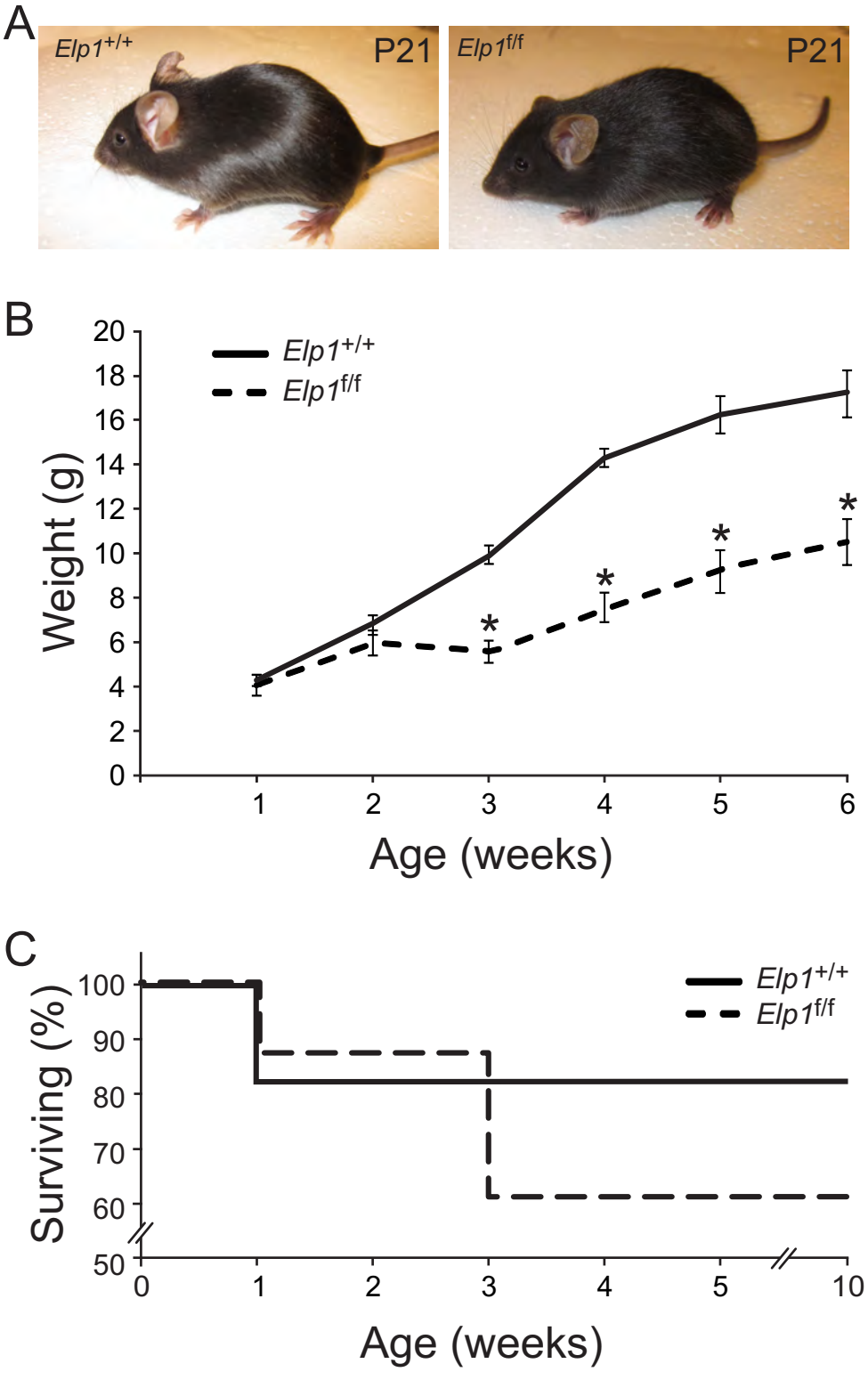

Elp1$^{f/f}$ mice were born at the expected Mendelean frequency and were viable. **(A)** By 3 weeks of age (P21), *Elp1*$^{f/f}$ mice appeared morphologically similar to *Elp1*$^{+/+}$ mice. **(B)** Within 1 week after birth their weights were similar, but by 3 weeks of age at the time of weaning, *Elp1*$^{f/f}$ mice weighed significantly less than *Elp1*$^{+/+}$ mice and the weight difference persisted after weaning (results represent > 75 mice, ANOVA for effect of genotype, $F_{1,78} = 107.0$, $p < 0.0001$, * = $p < 0.001$, Student's T test). **(C)** Within 1 week of age approximately 20% of *Elp1*$^{+/+}$ and *Elp1*$^{f/f}$ mice were lost in the colony due to normal attrition, but at P21, just after weaning, approximately 20% more *Elp1*$^{f/f}$ mice died relative to *Elp1*$^{+/+}$ mice, indicating that *Elp1*$^{f/f}$ mice have slightly increased postnatal mortality compared to *Elp1*$^{+/+}$ mice.

Supplementary Figure 2

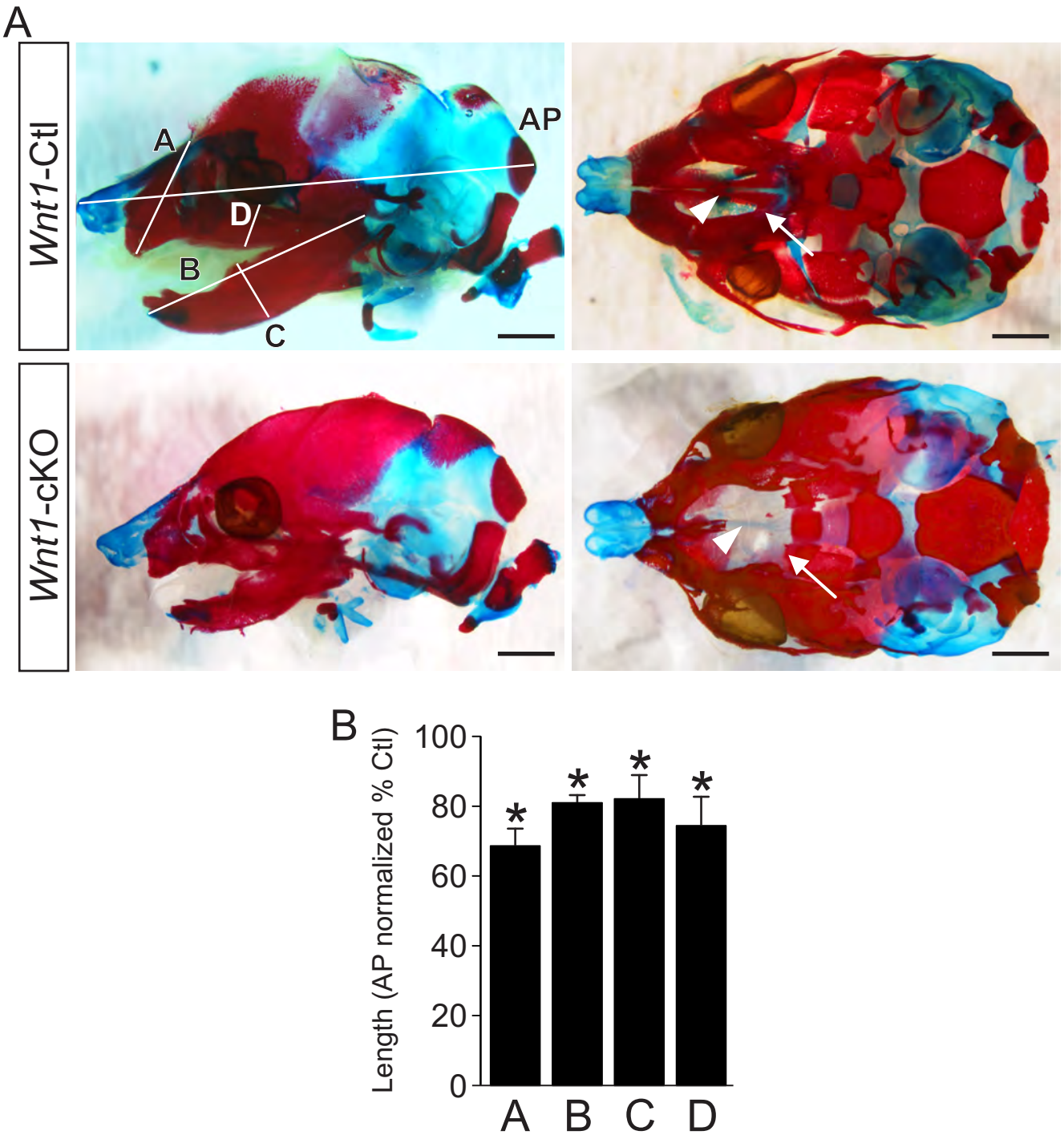

Alizarin red/Alcian blue staining of the skull from newborn *Wnt1*-Cre^{+};*Elp1*$^{f/f}$ (*Wnt1*-cKO) mice showed severe abnormalities of the palatal bones and mild craniofacial hypomorphisms. **(A)** In *Wnt1*-cKO mice the anterior portion of the maxilla, which forms the posterior limit of the hard palate, was absent (arrow) as was the Vomer bone which forms the central portion of the hard palate (arrowhead) (Scale = 0.5 cm). **(B)** Although most cranial bones appeared morphologically normal, there was mild skeletal hypomorphism in *Wnt1*-cKO mice indicated by comparatively small dimensions between skull landmarks (results represent percent mean ± SEM of selected skull dimensions in newborn *Wnt1*-cKO mice normalized to the overall AP length and then normalized to values obtained in *Wnt1*-Cre^{+};*Elp1*$^{+/+}$ (*Wnt1*-Ctl) mice, N=3 mice of each genotype analyzed; * = $p < 0.05$, Student's T test).

Supplementary Figure 3

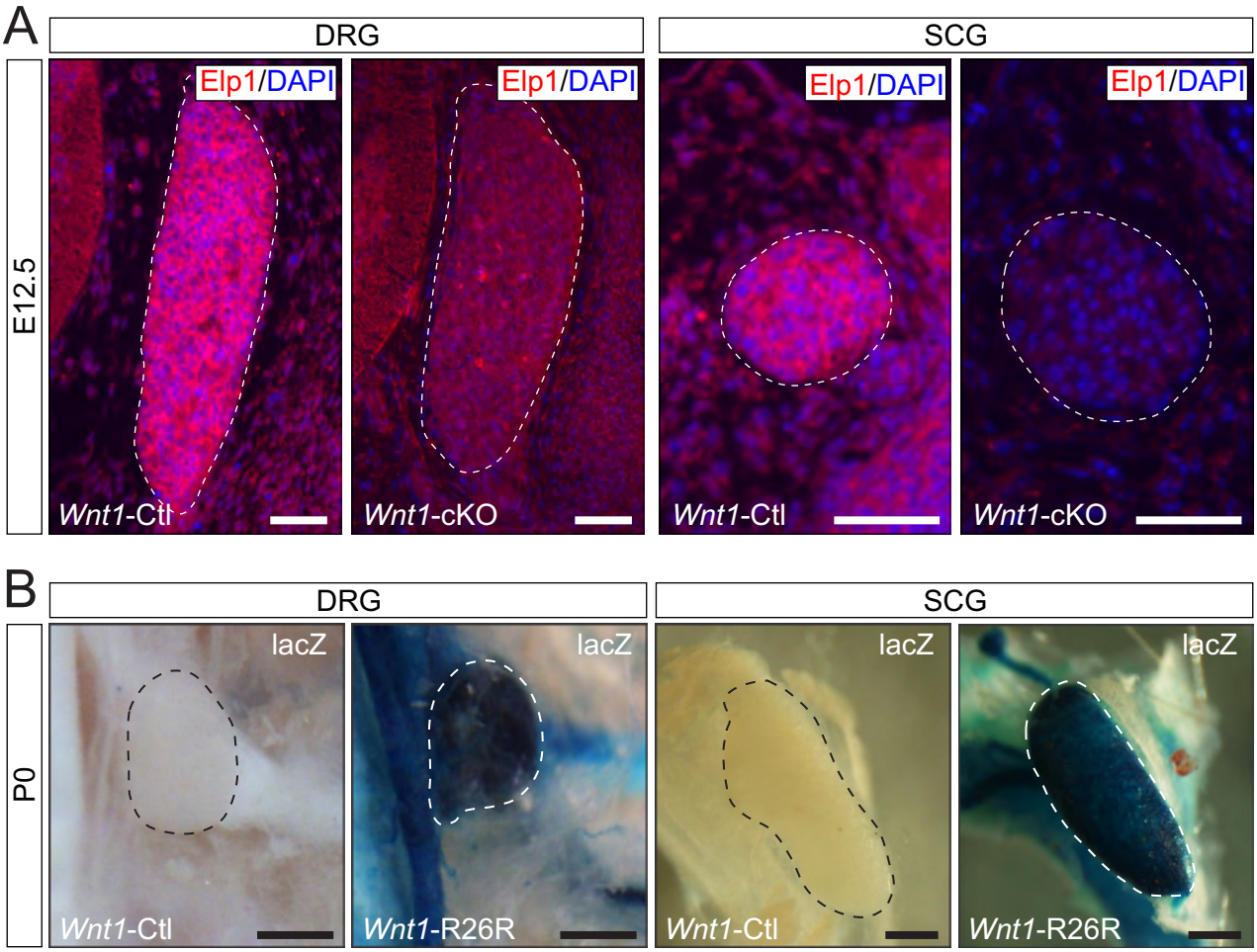

Wnt1-Cre driver mice efficiently ablated Elp1 and activated lacZ expression from the Rosa-26 (R26R) reporter allele in Wnt1-specified sympathetic and sensory neurons. **(A)** In embryonic day 12.5 (E12.5) mice, after most Wnt1-specified sympathetic and sensory neurons have completed migration and have coalesced into peripheral ganglia, Elp1 was efficiently ablated in *Wnt1*-cKO mice. Elp1, which is highly expressed in *Wnt1*-Ctl dorsal root ganglion (DRG) and superior cervical ganglion (SCG) neurons (Elp1 immunofluorescence, red and DAPI nuclear stain, blue) at E12.5 was completely absent in *Wnt1*-Cre^{+};*Elp1*$^{f/f}$ (*Wnt1*-cKO) SCG and DRG (Scale, 50 μm). **(B)** Similarly, P0 DRG and SCG neurons were strongly positive for blue lacZ reaction product generated by β-galactosidase (β-gal) expression as a marker of Wnt1 lineage-derived cells in *Wnt1*-Cre^{+};R26R$^{+/f}$ (*Wnt1*-R26R), but not *Wnt1*-Cre^{+};R26R$^{+/+}$ (*Wnt1*-Ctl) mice (Scale, 50 μm).

Supplementary Figure 4

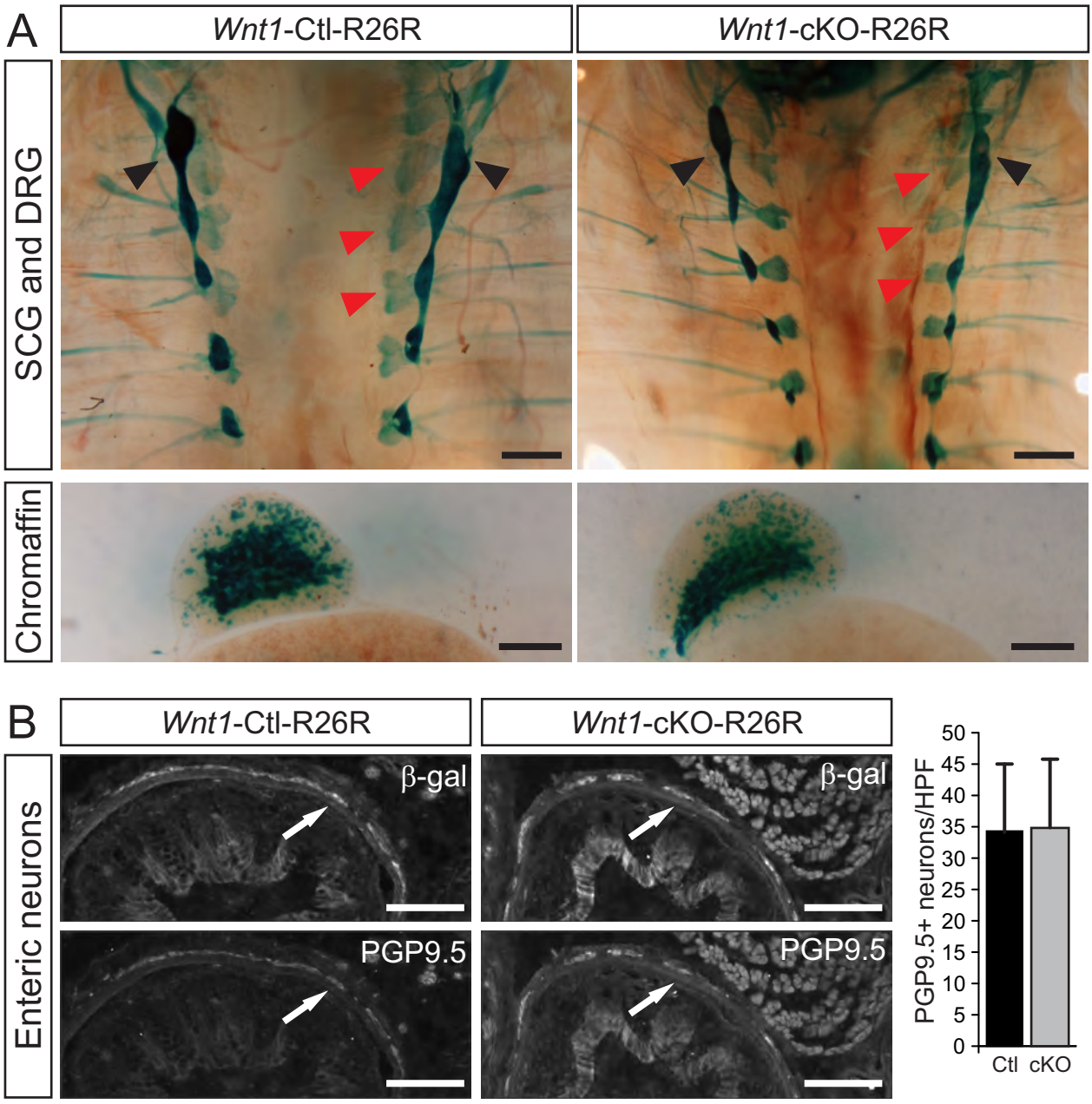

Wnt1 specified sympathetic neurons, sensory neurons, enteric neurons and adrenal chromaffin cells migrated normally from the neural crest in the absence of Elp1. **(A)** Wnt1-specified sympathetic, sensory and adrenal chromaffin cells were visualized using lacZ histochemistry from whole mount preparations of the cervical and thoracic body cavity and the adrenal glands from newborn *Wnt1*-Cre^{+};*Elp1*$^{+/+}$;R26R$^{+/f}$ or *Wnt1*-Cre^{+};*Elp1*$^{+/f}$;R26R$^{+/f}$ (*Wnt1*-Ctl-R26R) and *Wnt1*-Cre^{+};*Elp1*$^{f/f}$;R26R$^{+/f}$ (*Wnt1*-cKO-R26R) mice. The stellate ganglia (black arrowhead and sympathetic chain ganglia in foreground) as well as the DRG (red arrowheads, and ganglia in background) were properly positioned along the rostral-caudal axis, although they were smaller in *Wnt1*-cKO-R26R mice compared to *Wnt1*-Ctl-R26R mice. Similarly, chromaffin cells migrated to the adrenal gland medulla normally in the absence of Elp1 in *Wnt1*-cKO-R26R mice compared to *Wnt1*-Ctl-R26R mice (Scale, 500 μm top and 250 μm bottom). **(B)** Enteric neurons migrated to the gut normally in *Wnt1*-cKO-R26R mice. Sections of large bowel processed for immunohistochemistry showed enteric neurons that were labeled by the β-galactosidase (β-gal) reporter and the neuronal marker PGP9.5. Neuron migration was not altered as the number of enteric neurons were similar between *Wnt1*-cKO-R26R and Wnt1-Ctl-R26R mice (Scale, 500 μm, results represent mean ± SEM of neuron counts from N=2 mice of each genotype and > 30 sections analyzed; p = 0.88, Student's T test).

Supplementary Figure 5

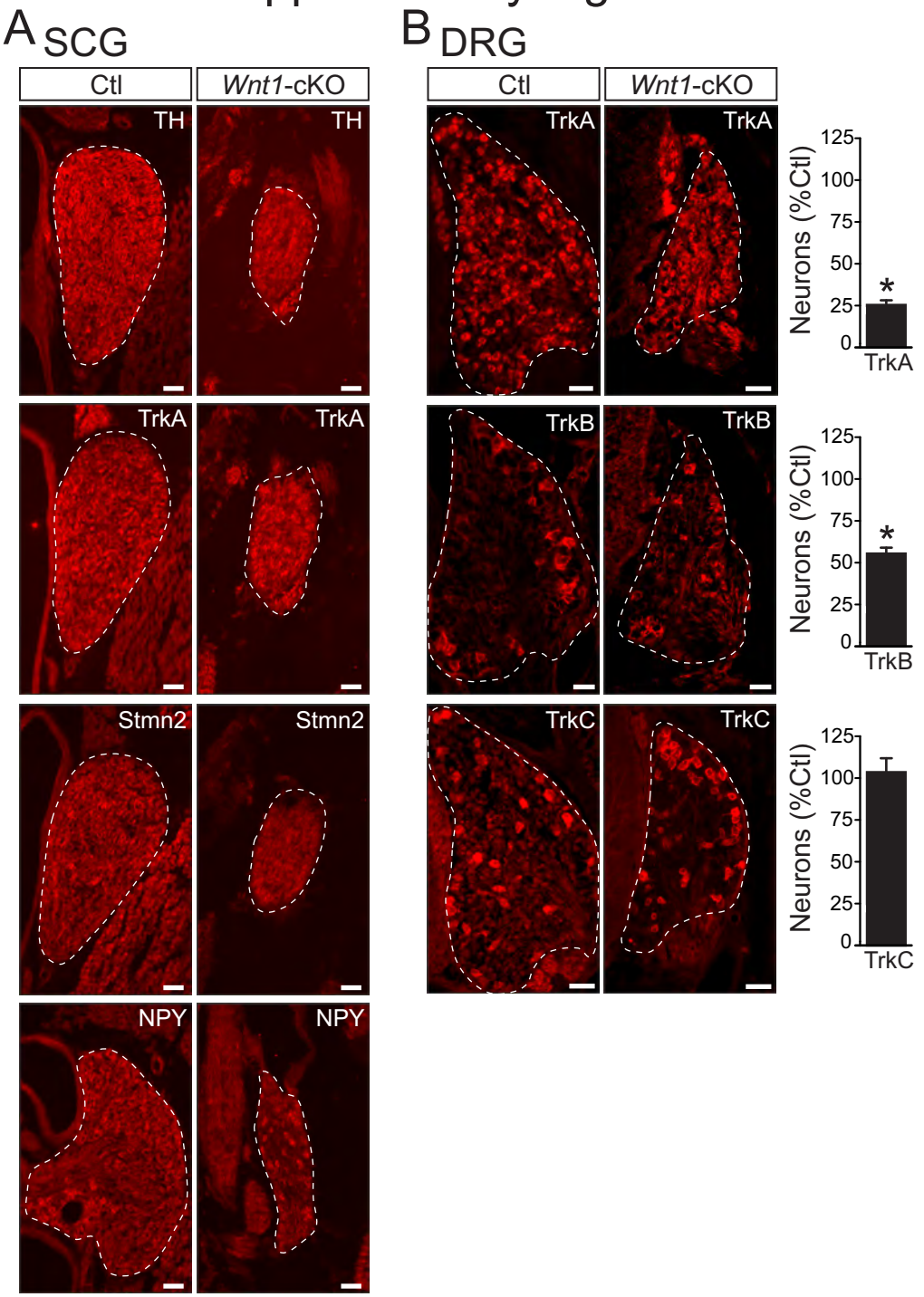

Normal sympathetic and sensory neuron differentiation in the absence of Elp1. **(A)** Although sympathetic ganglia, including the SCG, were smaller in *Wnt1*-Cre^{+};*Elp1*$^{f/f}$ (*Wnt1*-cKO) mice, they expressed sympathetic lineage-related proteins including tyrosine hydroxylase (TH), tropomyosin related kinase receptor A (TrkA), stathmin2 (Stmn2/SCG10) and neuropeptide Y (NPY) at levels similar to *Wnt1*-Cre^{+};*Elp1*$^{+/+}$ (*Wnt1*-Ctl) sympathetic neurons (Scale, 50 μm; immunofluorescence (red) for the protein indicated). **(B)** DRG sensory neurons also expressed characteristic sensory modality-associated proteins, including TrkA, TrkB and TrkC (immunofluorescence, red). Interestingly, both TrkA+ and TrkB+ neurons were reduced to 25% and 55% in *Wnt1*-cKO mice, respectively compared to *Wnt1*-Ctl mice, but TrkC+ neurons were not reduced in number. Loss of TrkA+ and TrkB+ neurons correlates with the small size of *Wnt1*-cKO ganglia compared to *Wnt1*-Ctl ganglia (Scale, 50 μm, results represent mean ± SEM of neuron counts from N=2-3 mice of each genotype; $p < 0.001$, Student's T test).

Supplementary Figure 6

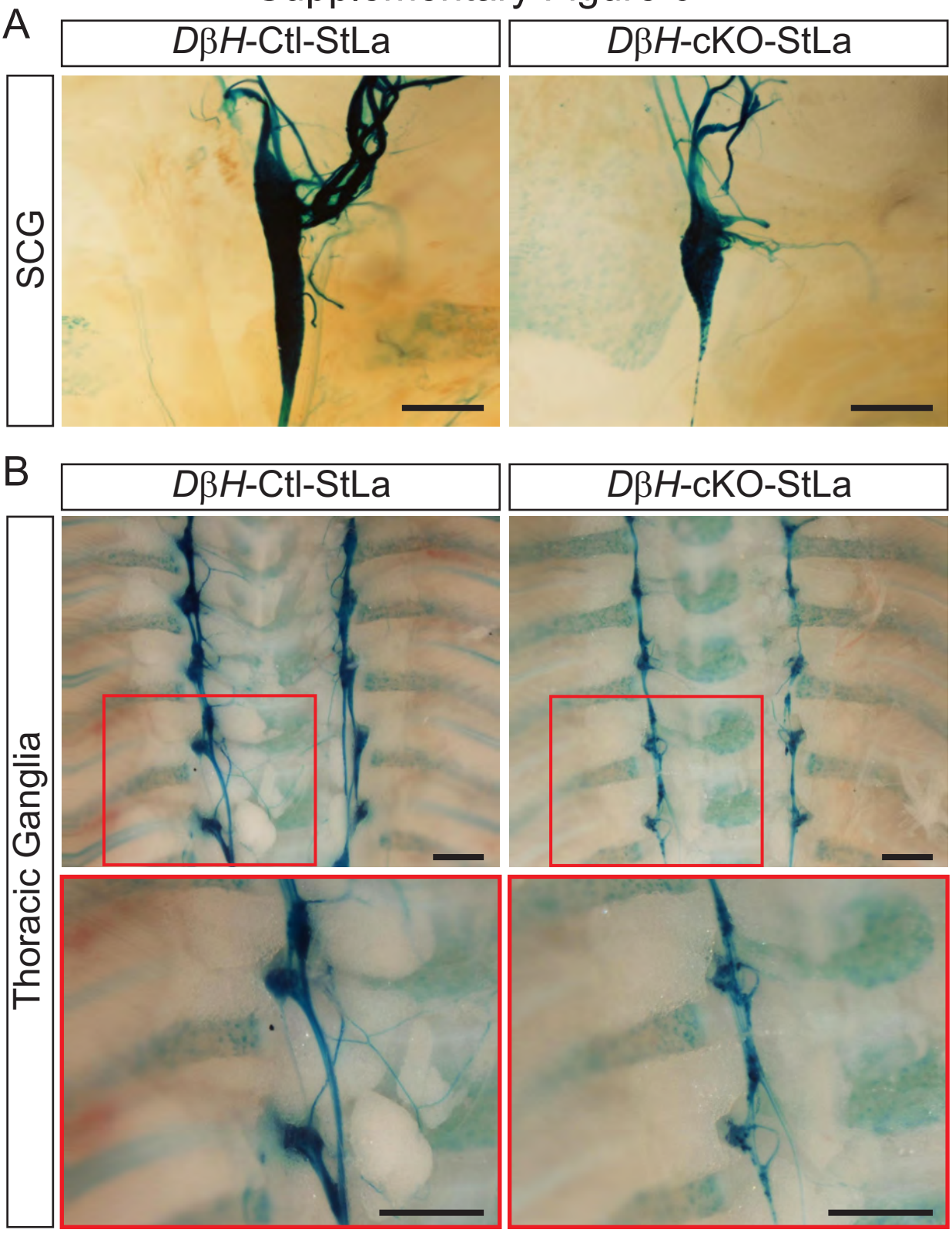

Elp1 has a sympathetic neuron autonomous function in their development and process outgrowth. Whole mount preparations and lacZ histochemistry in mice expressing the Cre-recombinase dependent axon localized β-galactosidase (lacZ) reporter allele (StLa) made it possible to visualize the entire chain of sympathetic ganglia and their proximal processes using *D*β*H*-iCre transgenic driver mice. The **(A)** SCG and **(B)** sympathetic chain ganglia were markedly smaller and had highly attenuated processes in *D*β*H*-iCre^{+};*Elp1*$^{f/f}$;StLa$^{+/f}$ (*D*β*H*-cKO-StLa) compared to *D*β*H*-iCre^{+};*Elp1*$^{+/+}$;StLa$^{+/f}$ (*D*β*H*-Ctl-StLa) mice (Scale,

Supplementary Figure 7

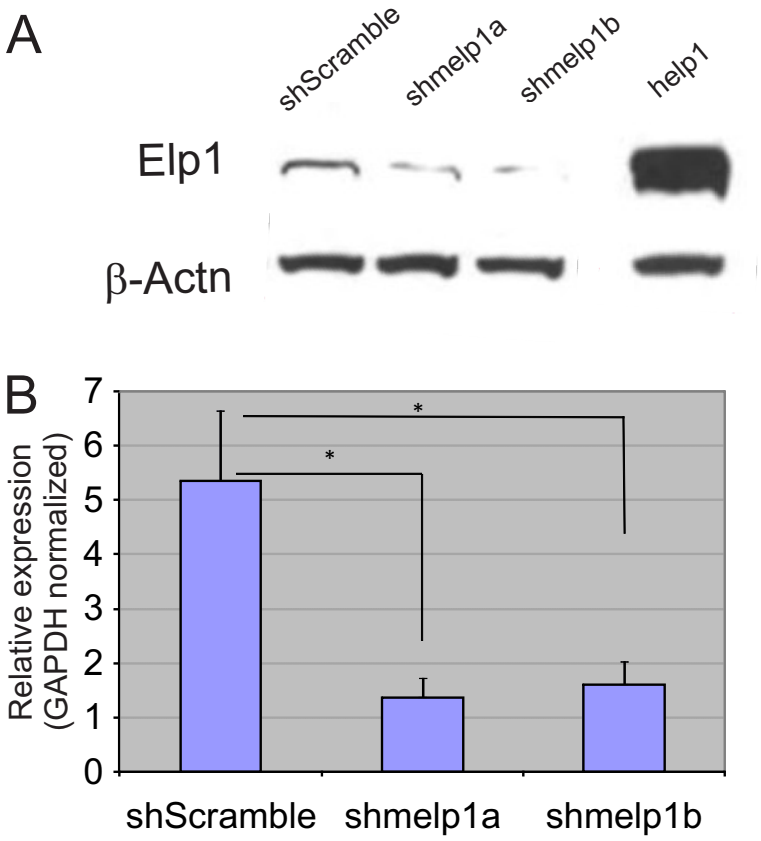

shRNA molecules that target elp1 are effective in reducing its expression in sympathetic neuron-derived N2a mouse neuroblastoma cells. **(A)** Western blot analysis for Elp1 using β-actin as protein loading control showed markedly reduced endogenous Elp1 by expression of shmelp1a or shmelp1b in N2a neuroblastoma cells. In addition, human Elp1 (help1) shRNA, which was not targeted by either shmelp1a or shmelp1b, was highly expressed in transfected N2a neuroblastoma cells. **(B)** Quantitative analysis showed approximately 25-30% reduction of endogenous Elp1 protein using either shmelp1a or shmelp1b (results represent mean ± SEM of densitometry values from Western blots performed in triplicate cell transfections; * = $p < 0.01$, Student's T test).

Supplementary Figure 8

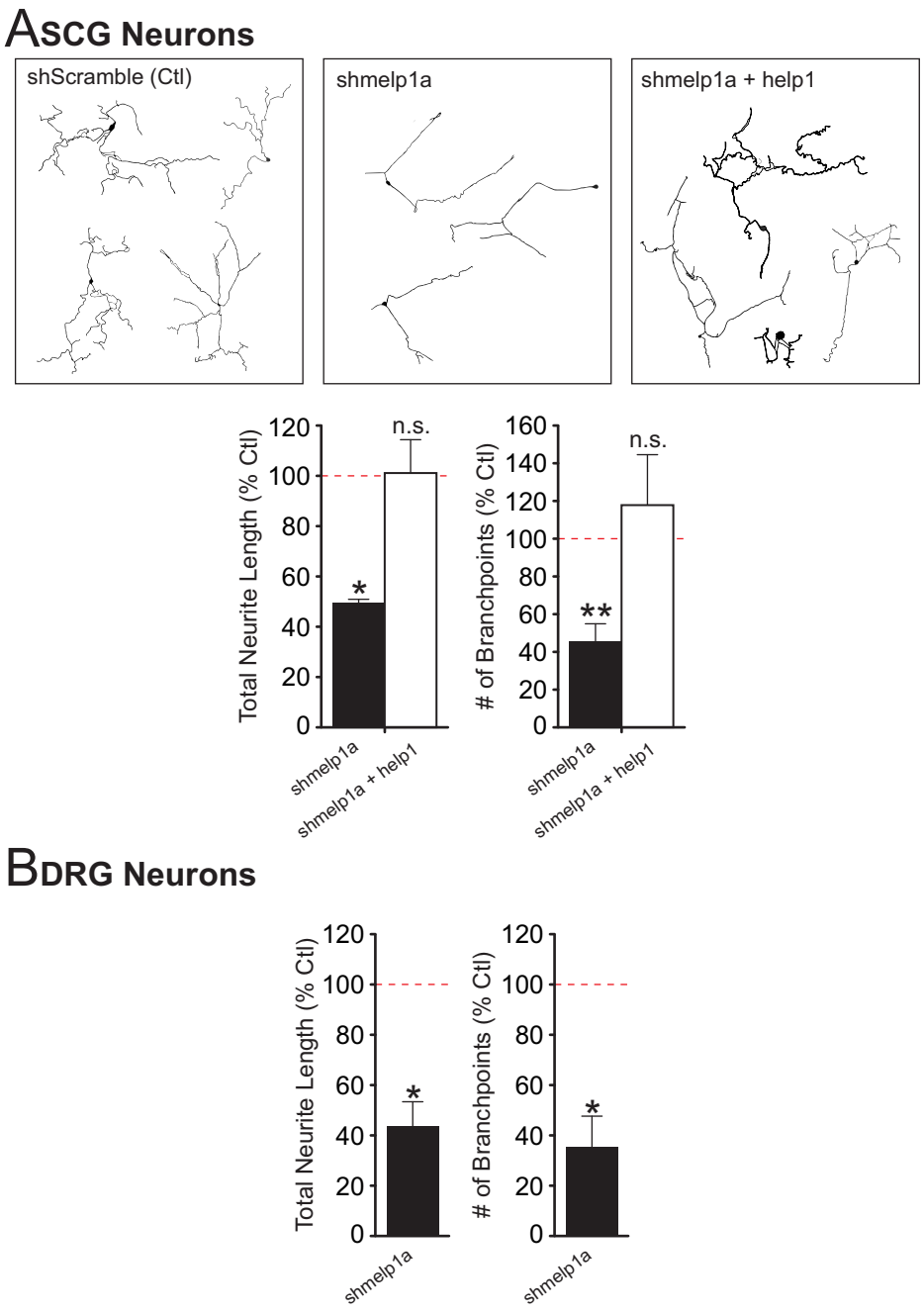

Reduction of endogenous Elp1 leads to a cell autonomous abnormality in neurite outgrowth and branching in primary mouse sympathetic and sensory neurons. **(A)** Relative to neurons transfected with the shScramble (Ctl) construct, neurons transfected with shmelp1a had significantly reduced neurite outgrowth (50% reduction compared to Ctl transfected neurons) and branching (52% reduction compared to Ctl transfected neurons). Moreover, neurite outgrowth and branching were rescued by expression of human elp1 (help1) that was unaffected by RNA degradation by shmelp1a (results represent mean ± SEM of triplicate experiments normalized to values obtained from Ctl transfected neurons, * = $p < 0.001$, Student's T test). **(B)** Similar results were obtained with transfected primary DRG sensory neurons that had significant reduction in neurite outgrowth (57% reduction compared to Ctl transfected neurons) and branching (62% reduction compared to Ctl transfected neurons) (results represent mean ± SEM of triplicate experiments normalized to values obtained from Ctl transfected neurons, * = $p < 0.001$, Student's T test).

Supplementary Movie 1

Wnt1-Cre^{+};*Elp1*$^{f/f}$ (*Wnt1*-cKO) mice die shortly after birth. They have labored breathing compared to *Wnt1*-Cre^{-};*Elp1*$^{+/+}$ (*Wnt1*-Ctl) mice.